Am J Transl Res 2024;16(12):7924-7936
www.ajtr.org /ISSN:1943-8141/AJTR0160816

Original Article

Heparan sulfate 6-O-sulfotransferase 2 promotes gastric cancer progression by modulating the TGF-β/smad2/3 pathway

Shuai Wu[1,2], Changqin Xu[3], Weijia Sun[4], Qianqian Xu[1], Feifei Zhou[3], Ruzhen Jia[3], Hongwei Xu[1,3]

[1]Department of Gastroenterology, Shandong Provincial Hospital, Shandong University, Jinan 250014, Shandong, China; [2]Department of Gastroenterology, The First Affiliated Hospital of Shandong First Medical University & Shandong Provincial Qianfoshan Hospital, Jinan 250014, Shandong, China; [3]Department of Gastroenterology, Shandong Provincial Hospital Affiliated to Shandong First Medical University, Jinan 250021, Shandong, China; [4]Center for Medical Integration and Practice, Shandong University, Jinan 250014, Shandong, China

Received September 27, 2024; Accepted December 3, 2024; Epub December 15, 2024; Published December 30, 2024

Abstract: Objective: To investigate the role of heparan sulfate 6-O-sulfotransferase 2 (HS6ST2) in gastric cancer (GC). Methods: HS6ST2 expression in GC and adjacent normal gastric mucosa was first detected via immunohistochemical (IHC) staining. The correlation between the expression level of HS6ST2 and clinicopathological parameters were observed. The protein expression of HS6ST2 in AGS, MKN45 and GES-1 cells was examined using Western blotting. The function of HS6ST2 in GC cells was explored via CCK-8, wound healing and Transwell assays. To elucidate the underlying molecular mechanisms, we detected whether HS6ST2 modulated the TGF-β/smad2/3 signaling pathway. Finally, we investigated the role of HS6ST2 in tumor growth in a nude mouse model. Results: The expression level of HS6ST2 in GC tissues was significantly higher than that in adjacent normal gastric mucosa and was positively correlated with tumor size. Compared with GES-1 cells, the expression level of HS6ST2 in AGS and MKN45 cells was significantly elevated. Silencing HS6ST2 impaired GC cell growth, mobility and epithelial-mesenchymal transition (EMT). On the other hand, HS6ST2 upregulation increased GC cell growth, migration and invasion, which was dramatically blocked by SB431542 treatment. Furthermore, mouse xenograft experiments demonstrated that HS6ST2 silencing inhibited tumor growth and EMT *in vivo*. Conclusion: HS6ST2 promotes GC progression through the modulation of the TGF-β/smad2/3 pathway.

Keywords: Epithelial-mesenchymal transition, gastric cancer, heparan sulfate 6-O-sulfotransferase 2, progression, TGF-β/smad2/3

Introduction

Gastric cancer (GC) is a malignant tumor originating from the gastric mucosa epithelium and it places a heavy burden on global health. Statistics show that there were more than 1 million new cases and approximately 769,000 deaths from GC worldwide in 2020 [1]. Having insidious early stage symptoms, lack of specific noninvasive diagnostic markers, low collective acceptance of gastroscopy contributes to a low diagnosis rate of gastric cancer, with a 5-year survival rate below 30% [2]. The exact mechanism underlying the development of GC is still not fully understood.

Heparan sulfate 6-O-sulfotransferase 2 (HS6ST2) is a member of the heparan sulfate sulfotransferase family, primarily responsible for catalyzing the transfer of a sulfate group from 3'-phosphoadenosine 5'-phosphosulfatesulfate (PAPS) to the 6-O position of the glucosamine residue in heparan sulfate proteoglycans (HSPGs) [3-5]. Heparan sulfate (HS) is a linear, sulfonated glycosaminoglycan widely present in the extracellular matrix, basement membrane, and cell surface [6]. HS interacts with different ligands and is involved in various cellular functions, such as cell growth, differentiation, adhesion, and migration [7]. After 6-O-sulfation, HS forms a three-molecule complex with growth

https://doi.org/10.62347/LWZR1836

factors and their receptors, which then promotes the occurrence and development of malignant tumors by stimulating cell proliferation and angiogenesis [8-10]. Many studies have confirmed that HS6ST2 plays a key role in the occurrence and development of various malignant tumors, including clear cell renal cell carcinoma [11, 12], lung cancer [13], colorectal cancer [14], pancreatic cancer [15], ovarian cancer [16], breast cancer [17] and cervical cancer [18]. Previous studies have shown that the overexpression of HS6ST2 is often associated with poor prognosis in GC patients [19]. However, the molecular biological functions and downstream signaling pathways of HS6ST2 in GC have not been fully elucidated. Therefore, this study aimed to investigate the role of HS6ST2 in the occurrence and progression of GC.

Materials and methods

Cell culture

AGS, MKN45 and the normal gastric epithelium cell line (GES-1) were purchased from ATCC, USA. The cell lines were cultured in RPMI 1640 medium (Gbico, USA) supplemented with 10% fetal bovine serum (Gbico, USA) in a humidified incubator with 5% CO_2 at 37°C.

Tissue microarray (TMA) and immunohistochemical analysis

TMA (#HStmA180Su18) containing 93 GC and 83 adjacent normal gastric mucosa samples (excluding damaged sections) was purchased from Shanghai Outdo Biotech (Shanghai, China). This study was approved by the Ethics Committee of Shanghai Outdo Biotech company. The TMA and paraffin-embedded subcutaneous tumors from nude mice were incubated with anti-HS6ST2 (Abcam, ab122220), anti-E-cadherin (ProteinTech, 20874), and anti-vimentin (ProteinTech, 10366) antibodies overnight and then washed with PBS (ServiceBio, Wuhan, China) 3 times for 5 min each. The mixture was gently shaken with PBS, the appropriate biotin-labeled goat anti-rabbit IgG was added, and the mixture was incubated at room temperature for 15 min. The staining results were scored in a blind manner by two senior pathologists. The IHC score was computed by multiplying the percentage of positive cells (1, ≤25%; 2, 26%-50%; 3, 51%-75%; 4, >75%) and the intensity of staining (0, negative staining; 1, weak staining; 2, moderate staining; 3, strong staining). The expression level of HS6ST2 can be classified into three different grades according to the IHC score: negative (score 0-3), weakly positive (score 4-8) and strongly positive (score 9-12).

Western blotting

Protein concentrations were determined using a protein concentration detection kit (Solarbio, PC0020). The protein marker (ABclonal, Wuhan, China) and 10-20 μg protein samples were added to the sample wells, separated via gel electrophoresis, and transferred to PVDF membranes. The membranes were blocked in 5% (w/v) fat-free dried milk powder in TBST (ServiceBio, Wuhan, China) at room temperature for 1-2 h. Primary antibodies were diluted according to the manufacturer's instructions, and the membranes were incubated overnight on a shaking bed at 4°C. The primary antibodies used included anti-HS6ST2 (1:500, Abcam, ab122220), anti-smad3 (phospho S423 + S425) (1:2000, Abcam, ab52903), anti-smad3 (1:2000, Abcam, ab40854), anti-smad2 (phospho S255) (1:2000, Abcam, ab188334), anti-smad2 (1:5000, ProteinTech, 67343-1-Ig), anti-E-cadherin (1:2000, ProteinTech, 20874-1-AP), anti-vimentin (1:2000, ProteinTech, 10366-1-AP), and anti-GAPDH (1:10000, ProteinTech, 60004-1-Ig). The secondary antibodies were selected according to the primary antibody species, and the membranes were incubated at room temperature for 1 h. All Western blotting Image strips were analyzed by grayscale scanning using ImageJ. The gray value of each protein band was calculated by multiplying the region by the mean gray value. The expression of the target protein was normalized by dividing the gray value of the target protein by the gray value of the internal reference protein.

Cell transfection

Lentiviruses expressing HS6ST2 cDNA and HS6ST2 short hairpin RNA (shRNA), with sequences provided in Table S1 were synthesized by Beijing Syngentech Co., Ltd. (Beijing, China). GC cell lines were seeded in 24-well plates at 1×10^4 cells/well, cultured at 37°C for 16-24 hours. Lentiviral infection was performed when the cell confluence was about 20-30%. The virus stock solution was diluted using complete medium containing polybrene and added into the corresponding cells. The cells were cultured at 37°C for 8 to 12 hours. After 48 to 72

hours of lentiviral infection (70-80% fusion), complete culture medium containing purinomycin (Genechem, Shanghai, China) was added to screen successfully transfected cells. After 2 weeks of continuous screening, stably lentivirus-transfected cell lines were obtained. Western blotting was used to determine the transfection efficacy.

CCK-8 assay

The cells were seeded into 96-well plates at a density of 3000 cells per well. Cell Counting Kit 8 (CCK-8) (ProteinTech, PF00004) reagent was added to each well every 24 h, and the samples were incubated for 2 h. Absorbance was measured at 450 nm using a microplate reader (Thermo Fisher, USA).

Wound healing assay

Straight lines were drawn evenly on the back of the 6-well plates. Cells in the logarithmic growth stage were cultured at a density of 1×10^6 cells/well until the cell density reached more than 70%. Cell scratches with uniform force were created via a 200 μL pipette tube. The original medium was removed and discarded, and the cells were washed with sterile PBS several times to remove floating cells. Serum-free medium was added to continue the culture. Photos were taken 0 and 48 hours after the lines were crossed.

Cell invasion and migration assays

A single-cell suspension was prepared from cells in the logarithmic growth phase, and the cell density was adjusted to 2×10^5 cells/ml in serum-free medium. Then, 600 μL of medium containing 10% fetal bovine serum was added to the lower chamber of a 24-well plate. The Transwell chamber (Costar, Corning, NY, USA) coated with or without Matrigel (BD, Franklin Lakes, USA) was used to assess invasion or migration ability. One hundred microliters of cell suspension was seeded in the upper chamber and cultured for 24 hours. Next, 500 μL of 4% paraformaldehyde (ServiceBio, Wuhan, China) was added to the lower chamber of the Transwell for 10 min, and 500 μL of 0.1% crystal violet solution was added for 20 min. The cells in the upper chamber were removed with a cotton swab, and the mixture was air dried at room temperature. The capsule membrane was cut, placed on a slide, and then sealed with neutral gum. Five random fields were observed under a high-power microscope (Olympus, Japan), and the cells were counted for statistical analysis.

Xenograft model

This study was approved by the Experimental Animal Ethics Committee of Shandong Provincial Hospital. Sixteen six-week-old female nude mice from Beijing Vital River Laboratory Animal Technology Co., Ltd. (Beijing, China) were randomly divided into two groups (8 mice in each group). The temperature of the animal house was maintained at 22±2°C and the relative humidity was maintained at 50%±10%. Approximately 1×10^7 MKN45-sh-NC or MKN45-sh-HS6ST2 cells were injected into the axillary region of nude mice from the two groups separately. Tumor volume and body weight of the nude mice were measured every 3 days after implantation. After 21 days of observation, the mice were sacrificed, and blood was collected from the heart after intraperitoncal injection of tribromoethanol at a dosage of 280 mg/kg. Tumors were dissected and weighed. Some of the tumors were frozen in liquid nitrogen immediately, while the rest were fixed in formalin solution for subsequent HE and IHC staining.

Statistical analysis

The images were analyzed with ImageJ, and the data were statistically analyzed with GraphPad Prism 10 software. Each experiment was repeated at least three times, and the measurements were expressed as means ± standard deviations. Two-tailed *t* tests were used for comparisons between two independent samples, while Tukey's post hoc test after one-way analysis of variance (ANOVA) was used to compare the differences among multiple groups. Count data were expressed as n (%) and was analyzed via the X^2 test. A *P* value <0.05 was considered statistically significant, denoted as $*P<0.05$ and $**P<0.01$ in the figures.

Results

Higher expression of HS6ST2 in GC tissues and cell lines

HS6ST2 expression in 83 pairs of GC and adjacent normal gastric mucosa samples from the TMA was examined via immunohistochemical

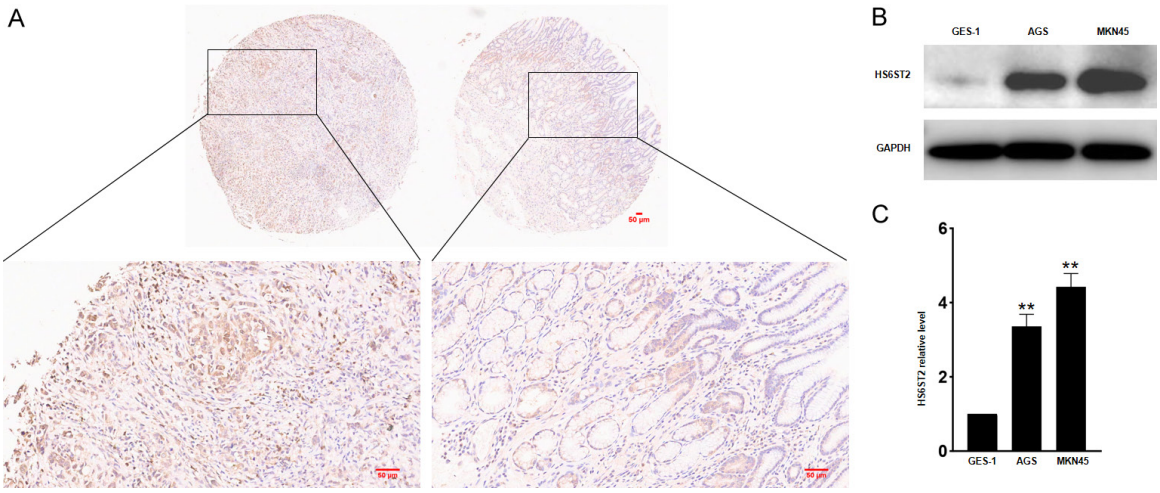

Figure 1. HS6ST2 expression was upregulated in gastric cancer (GC) tissues and cell lines. A. Representative images of immunohistochemical (IHC) staining for HS6ST2 in 83 pairs of GC (left) and adjacent tissues (right) from tissue microarray; Scale bar = 50 μm. B and C. HS6ST2 expression was significantly increased in AGS and MKN45 cell lines compared with the normal gastric epithelial cell line GES-1. The intensity of the Western blot bands was quantified by scanning densitometry. All experiments were repeated at least three times. Data are expressed as mean ± SD, **P<0.01 (ANOVA).

Table 1. Upregulated HS6ST2 expression in gastric cancer tissues compared with adjacent non-tumor tissues

	All cases	Negative	Weakly positive	Strongly positive
Adjacent tissues	83	15	37	31
GC	83	0	28	55
P value <0.0001				

X^2 test was used for statistical analysis.

staining. The results revealed upregulated HS6ST2 expression in GC compared with adjacent normal gastric mucosa (**Figure 1A** and **Table 1**). We further evaluated whether the expression level of HS6ST2 was correlated with the clinicopathological parameters of 93 patients with GC from the TMA. Statistical studies revealed that HS6ST2 expression was positively correlated with tumor size but not significantly correlated with other clinicopathological parameters of GC patients (**Table 2**). Our study further investigated HS6ST2 expression in AGS, MKN45 and GES-1 cells via Western blotting. We found that the expression level of HS6ST2 in AGS and MKN45 cells was significantly greater than that in GES-1 cells (**Figure 1B** and **1C**).

HS6ST2 silencing inhibited GC cell growth, invasion, migration and EMT

We generated stable HS6ST2-knockdown AGS and MKN45 (**Figure 2A-D**) cell lines via lentiviral-based shRNA delivery. Among the three distinct HS6ST2 shRNA sequences tested, shRNA-1 demonstrated the most potent knockdown effect in both cell lines. Therefore, HS6ST2 shRNA-1 was chosen for subsequent experiments. To investigate the function of HS6ST2 in GC cells, we performed a series of cell function experiments. In the CCK-8 assay, the downregulation of HS6ST2 significantly inhibited the proliferation of AGS (**Figure 2E**) and MKN45 (**Figure 2F**) cells. Compared with control cells, cells transfected with HS6ST2 shRNA displayed delayed wound closure (**Figure 2G-J**). Downregulation of HS6ST2 in AGS and MKN45 cells also reduced cell migration and invasion ability in the Transwell assay (**Figure 3A-D**). We investigated whether the expression of E-cadherin and vimentin, which are important markers of EMT, was affected by the expression of HS6ST2. After HS6ST2 silencing in AGS and MKN45 cells, the expression of E-cadherin increased and vimentin decreased (**Figure 3E** and **3F**), whereas the opposite

Table 2. Correlation between HS6ST2 expression and the clinicopathological characteristics of gastric cancer

	Cases (n)	Negative or weakly positive	Strongly positive	*P* value
Gender				0.1271
Male	54	15	39	
Female	39	17	22	
Age				0.5138
≤60	39	15	24	
>60	54	17	37	
Degree of differentiation				0.8171
High	63	21	42	
Moderate/poor	30	11	19	
Tumor size (cm)				0.0462
<5	36	17	19	
≥5	57	15	42	
Tumor site				0.0709
Upper	11	3	8	
Middle	33	16	17	
Lower	46	11	35	
Diffuse	3	2	1	
Depth of Invasion				0.5459
pT1 + 2	14	6	8	
pT3 + 4	79	26	53	
Lymph node				0.2112
Negative	22	5	17	
Positive	71	27	44	
Distant metastasis				>0.9999
No	89	31	58	
Yes	4	1	3	
TNM stage				0.5076
I/II	37	11	26	
III/IV	56	21	35	

X^2 test was used for statistical analysis.

changes occurred after HS6ST2 overexpression (**Figure 3G** and **3H**). Collectively, these findings suggested that the downregulation of HS6ST2 impaired the growth, mobility and EMT of GC cells.

HS6ST2 promoted GC progression via TGF-β/smad2/3 signaling

To clarify the downstream signaling pathway by which HS6ST2 mediates its oncogenic functions in GC, we detected whether HS6ST2 modulates the TGF-β/smad2/3 signaling pathway, which is frequently aberrantly activated in human cancers. Interestingly, we found that the downregulation of HS6ST2 markedly decreased the phosphorylation of smad2/3, whereas the expression of total smad2/3 did not significantly change (**Figure 4A** and **4B**). In contrast, the upregulation of HS6ST2 induced the phosphorylation of smad2/3 (**Figure 4C** and **4D**). Our findings revealed that HS6ST2 positively modulates TGF-β/smad2/3 signaling *in vitro*. We further studied whether HS6ST2 could facilitate GC cell growth and mobility via TGF-β/smad2/3 signaling. We found that overexpressed HS6ST2 increased GC cell growth, migration and invasion, which were prominently reversed by treatment with the TGF-β/smad2/3 pathway inhibitor SB431542 (**Figure 5A-F**). Thus, these data suggest that HS6ST2 might regulate GC cell progression at least partially through the modulation of the TGF-β/smad2/3 pathway.

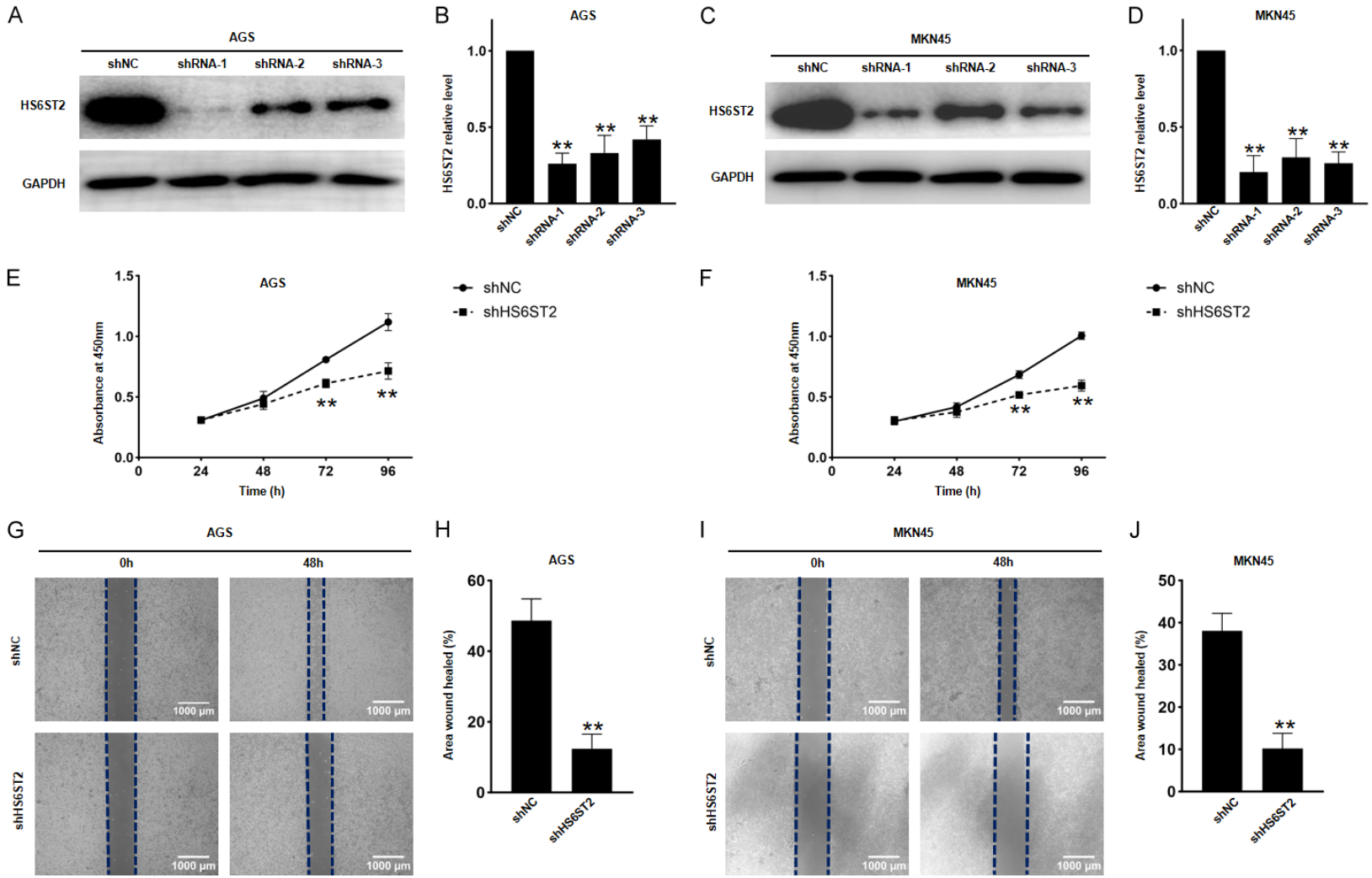

Figure 2. HS6ST2 knockdown inhibited the growth and wound closure of AGS and MKN45 cells. (A-D) Western blot analysis confirmed stable HS6ST2 knockdown in both AGS (A and B) and MKN45 (C and D) cell lines using lentiviral-based shRNA delivery. (E and F) HS6ST2 knockdown inhibited the growth of AGS (E) and MKN45 (F) cells determined by CCK-8 assay. (G-J) The wound healing assays showed that knockdown of HS6ST2 displayed delayed wound closure of the GC-derived cell lines AGS (G and H) and MKN45 (I and J); Scale bar = 1000 μm. All experiments were repeated at least three times. Data are expressed as mean ± SD, **P<0.01 (*t*-test).

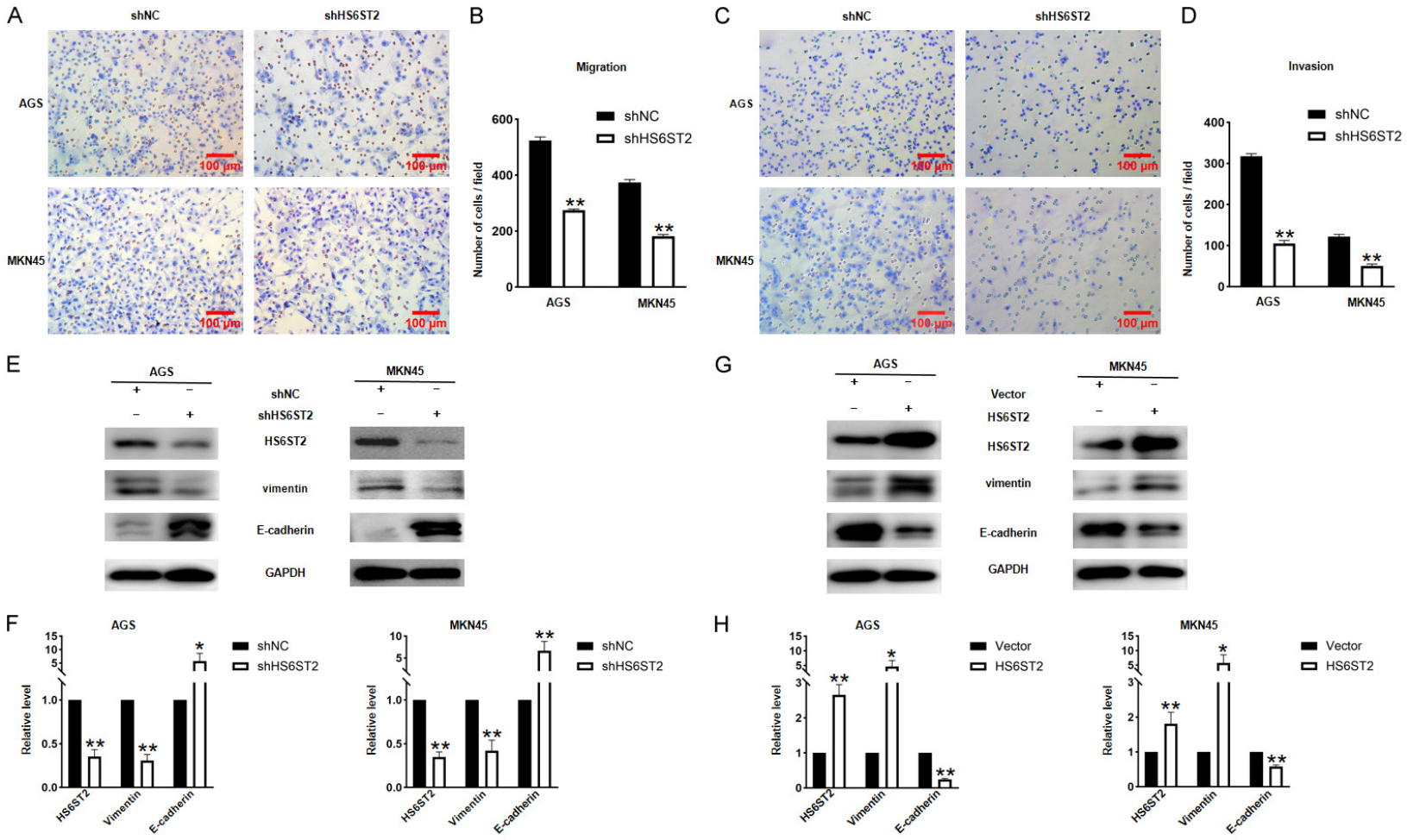

Figure 3. Down-regulation of HS6ST2 reduced migration and invasion of gastric cancer cells. (A-D) Decreased migratory (A and B) and invasive (C and D) abilities of AGS and MKN45 cells after HS6ST2 down-regulation; Scale bar = 100 μm. (E-H) The expression vimentin and E-cadherin determined using Western blotting in AGS and MKN45 cells after silence (E and F) and overexpression (G and H) of HS6ST2 respectively. All experiments were repeated at least three times. Data are expressed as mean ± SD, **P<0.01 (*t*-test).

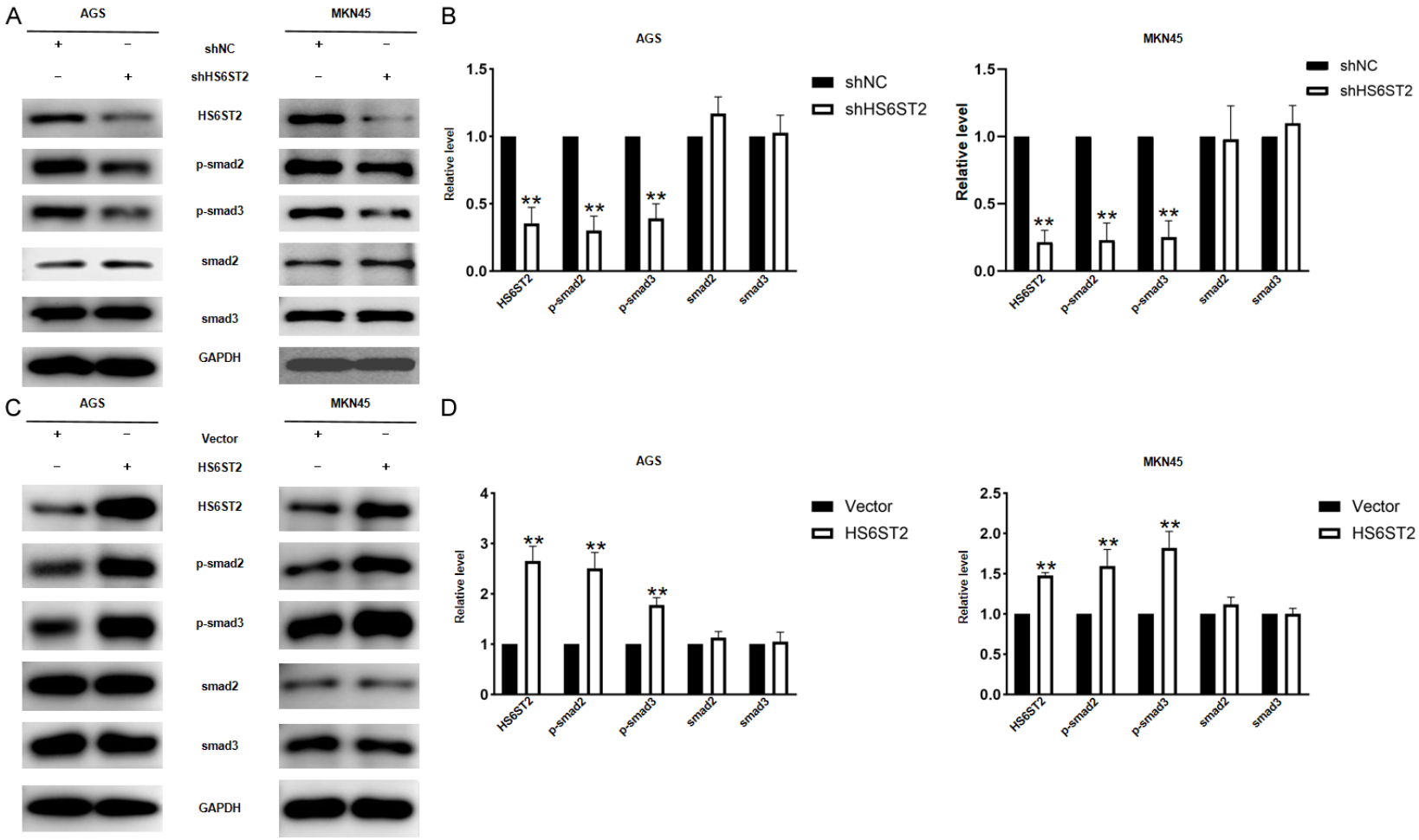

Figure 4. HS6ST2 positively modulated TGF-β/smad2/3 signaling pathway in vitro. A and B. Knockdown of HS6ST2 dramatically reduced the phosphorylation of smad2 and smad3 in both AGS and MKN45 cells; however, no detectable changes in the total levels of smad2 and smad3 were observed. C and D. Ectopic overexpression of HS6ST2 increased the phosphorylation of smad2 and smad3 in both AGS and MKN45 cells. All experiments were repeated at least three times. Data are expressed as mean ± SD, **P<0.01 (*t*-test).

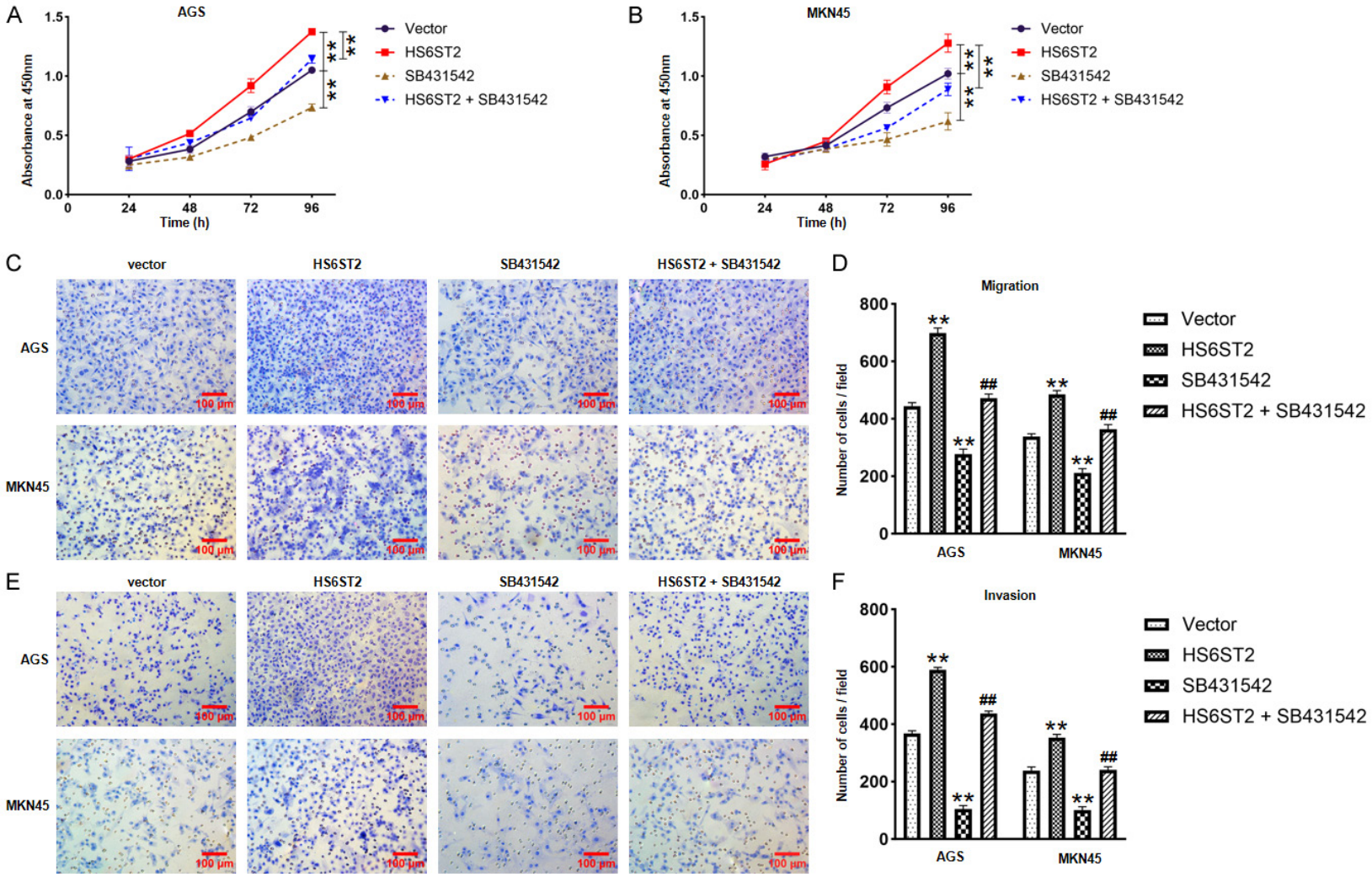

Figure 5. HS6ST2 promoted cancer cell proliferation, migration and invasion via TGF-β/smad2/3 signaling. Overexpression of HS6ST2 promoted cell proliferation (A and B), migration (C and D) and invasion (E and F) in GC cells, while this change was dramatically blocked after TGF-β/smad2/3 pathway inhibitor SB431542 treatment; Scale bar = 100 μm. All experiments were repeated at least three times. Data are expressed as mean ± SD, **P<0.01, compared with vector group. ##P<0.01, compared with HS6ST2 group (ANOVA).

Downregulation of HS6ST2 inhibited tumor growth and EMT in vivo

We investigated the role of HS6ST2 in tumor growth via a nude mouse model. HS6ST2 silencing inhibited tumor size, tumor growth and tumor weight, whereas the body weights of the nude mice did not change significantly (**Figure 6A-D**). Furthermore, the xenograft tumor HE and IHC staining results demonstrated that the expression of E-cadherin increased, and Ki-67 and vimentin decreased after the downregulation of HS6ST2 (**Figure 6E** and **6F**). Together, these results showed that HS6ST2 silencing inhibited tumor growth and EMT *in vivo*.

Discussion

Gastric cancer (GC) is a prevalent cancer that threatens human health. Early diagnosis remains challenging, and the prognosis is generally poor [20]. Although the development of multimodal treatment, including surgery combined with systemic chemotherapy, has improved patient survival, the overall survival rate remains low [21]. In recent years, molecular targeted therapy has shown good clinical efficacy and broad application prospects [22, 23]. Therefore, new and accurate target molecules for the early diagnosis and targeted therapy of GC are urgently needed.

HS6ST2 is a Golgi-resident enzyme that catalyzes the transfer of sulfate groups from adenosine 3'-phosphate and 5'-phosphate to the C-6 position of glucosamine residues in HSPGs. Heparan sulfate (HS) is a macromolecular polysaccharide widely present in the extracellular matrix and cell membrane [6]. It interacts with many ligands and plays important roles in cell growth, differentiation, adhesion, and migration [7]. The specificity of HS binding to its ligands depends largely on the abundance and arrangement of sulfate groups in the different structural motifs. Researchers have demonstrated that HS6ST2 regulates the progression and EMT process of many tumors [15, 24]. However, the functions and downstream signaling pathways of HS6ST2 in GC have not been fully clarified.

In this study, we observed upregulated HS6ST2 expression in GC tissues compared with adjacent normal gastric mucosa via a TMA, which is consistent with the findings of previous studies [19]. Moreover, there was a positive correlation between HS6ST2 expression and tumor size in GC patients. These findings suggest that HS6ST2 might play an important role in GC progression. The Western blot results revealed that the expression of HS6ST2 in AGS and MKN45 cells was significantly higher than that in GES-1 cells. When HS6ST2 expression was suppressed in AGS and MKN45 cells, a marked decrease in cell proliferation was observed. In agreement with the *in vitro* results, HS6ST2 silencing also inhibited tumor growth *in vivo*. In the wound healing assay, compared with control cells, HS6ST2-knockdown cells displayed delayed wound closure. Similarly, in the Transwell assay, the downregulation of HS6ST2 significantly reduced cell migration and invasion ability. This phenomenon can also be seen in previous reports of cervical cancer [18]. EMT enables cancer cells to acquire mesenchymal characteristics, including increased motility and decreased intercellular adhesion, which is an important step in tumor progression [25, 26]. E-cadherin and vimentin are important markers of EMT [27, 28], and the results revealed that the expression of E-cadherin was increased and vimentin was decreased in GC cells after the silencing of HS6ST2, whereas the opposite results were obtained after the overexpression of HS6ST2. Consistently, HS6ST2 knockdown dramatically increased the expression of E-cadherin and decreased the expression of Ki-67 and vimentin in xenograft tumors. In summary, HS6ST2 plays a pivotal role in promoting the growth, motility and EMT of GC cell lines.

To understand the molecular basis of the role of HS6ST2 in GC, we performed Western blot analysis to investigate the signaling pathways affected by HS6ST2 expression. Previous research confirmed that HS6ST2 is critical for IL-11 induction by TGF-β in breast cancer cells [17]. Interestingly, we found that HS6ST2 depletion impaired the phosphorylation of smad2/3, whereas ectopic overexpression of HS6ST2 induced the activation of smad2/3, crucial components of TGF-β/smad2/3 signaling [29, 30]. Moreover, the HS6ST2-induced increase in GC cell growth, migration and invasion was prominently reversed by treatment with the TGF-β/smad2/3 pathway inhibitor SB431542 [31, 32]. Thus, these data demonstrated that HS6ST2 promoted GC progression partially by regulating the TGF-β/smad2/3 pathway, which

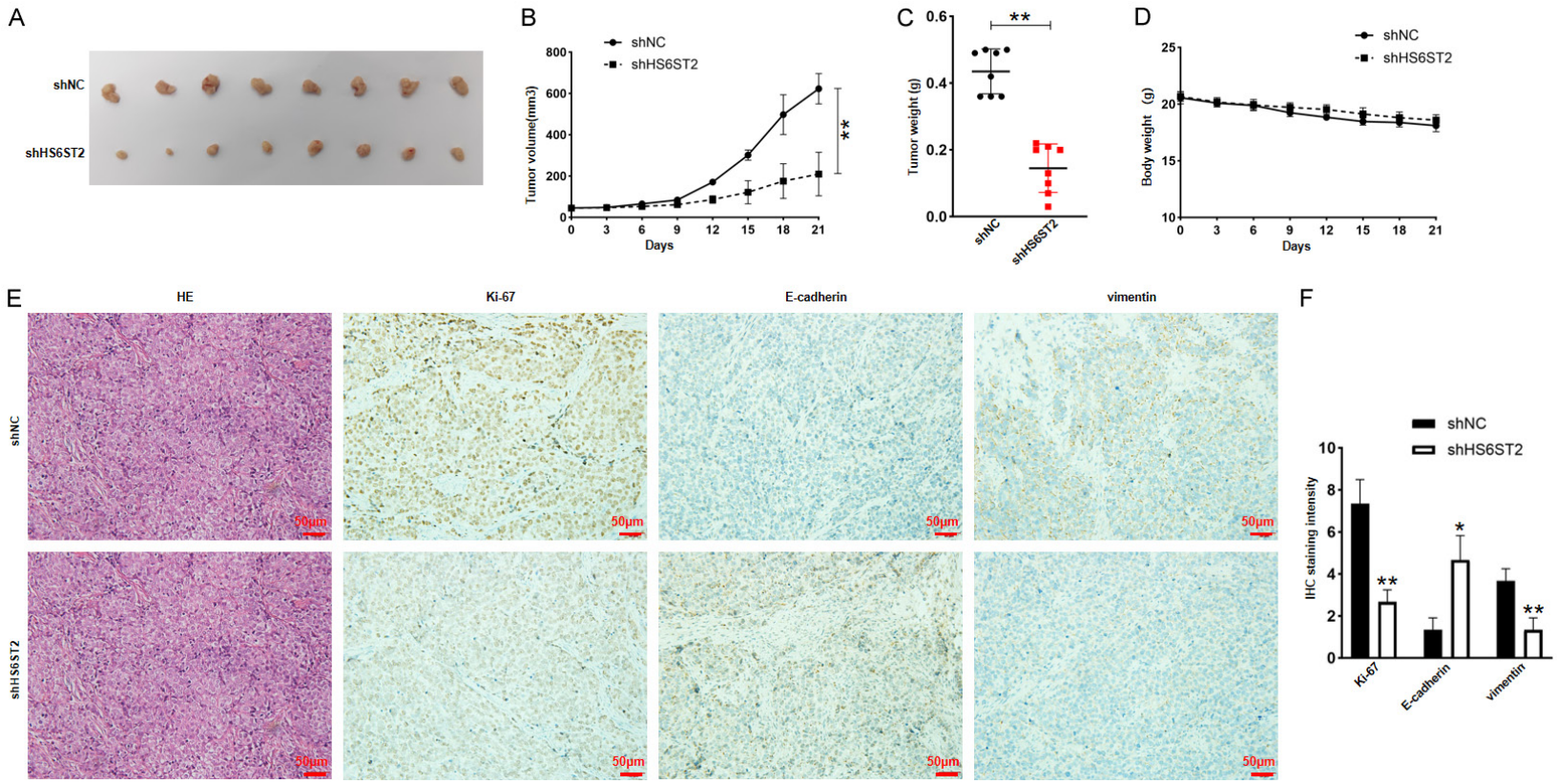

Figure 6. Silencing of HS6ST2 inhibited the growth of gastric cancer in vivo. Representative tumor images (A), tumor growth curve (B), tumor weight (C) and body weight (D) of MKN45-sh-NC and MKN45-sh-HS6ST2 group (n = 8 mice). (E and F) IHC analysis of vimentin, E-cadherin and Ki-67 expression in xenograft tumor issues; Scale bar = 50 μm. Data are expressed as mean ± SD, *P<0.05, **P<0.01 (*t*-test).

is frequently aberrantly activated in human cancers [33-35]. This is not exactly consistent with previous studies of HS6ST2 in pancreatic cancer, which found that silencing of hHS6ST2 inhibited progression of pancreatic cancer through inhibition of Notch signaling [15], suggesting that HS6ST2 might play a regulatory role in a variety of signaling pathways.

Our research still has several limitations. The clinical sample size can be further expanded, and the correlation of HS6ST2 to the prognosis and survival of patients with GC can be further studied. Clarifying the direct and precise link between HS6ST2 and the TGF-β/smad2/3 pathway is highly important for future studies. Nevertheless, our findings reveal the molecular biological functions and downstream signaling pathways of HS6ST2 in GC, which has important implications for identifying potential therapeutic targets for GC in the future.

In conclusion, HS6ST2 is highly expressed in GC tissues. HS6ST2 promotes GC progression through modulation of the TGF-β/smad2/3 pathway. Future preclinical investigations are needed to validate our findings and explore the therapeutic potential of targeting HS6ST2 in GC.

Acknowledgements

This work is supported by the National Natural Science Foundation of China [82170650].

Disclosure of conflict of interest

None.

Address correspondence to: Hongwei Xu, Department of Gastroenterology, Shandong Provincial Hospital, Shandong University; Shandong Provincial Hospital Affiliated to Shandong First Medical University, No. 324, Jingwuweiqi Road, Jinan 250021, Shandong, China. Tel: +86-0531-6887-6350; E-mail: xhwsdslyy@126.com

References

[1] Sung H, Ferlay J, Siegel RL, Laversanne M, Soerjomataram I, Jemal A and Bray F. Global Cancer Statistics 2020: GLOBOCAN estimates of incidence and mortality worldwide for 36 cancers in 185 countries. CA Cancer J Clin 2021; 71: 209-249.

[2] Thrift AP and El-Serag HB. Burden of gastric cancer. Clin Gastroenterol Hepatol 2020; 18: 534-542.

[3] Habuchi H, Tanaka M, Habuchi O, Yoshida K, Suzuki H, Ban K and Kimata K. The occurrence of three isoforms of heparan sulfate 6-O-sulfotransferase having different specificities for hexuronic acid adjacent to the targeted N-sulfoglucosamine. J Biol Chem 2000; 275: 2859-2868.

[4] Sasisekharan R, Shriver Z, Venkataraman G and Narayanasami U. Roles of heparan-sulphate glycosaminoglycans in cancer. Nat Rev Cancer 2002; 2: 521-528.

[5] Huang L, Irshad S, Sultana U, Ali S, Jamil A, Zubair A, Sultan R, Abdel-Maksoud MA, Mubarak A, Almunqedhi BM, Almanaa TN, Malik A, Alamri A, Kodous AS, Mares M, Zaky MY, Saba Sajjad S and Hameed Y. Pan-cancer analysis of HS6ST2: associations with prognosis, tumor immunity, and drug resistance. Am J Transl Res 2024; 16: 873-888.

[6] Bernfield M, Götte M, Park PW, Reizes O, Fitzgerald ML, Lincecum J and Zako M. Functions of cell surface heparan sulfate proteoglycans. Annu Rev Biochem 1999; 68: 729-777.

[7] Esko JD and Lindahl U. Molecular diversity of heparan sulfate. J Clin Invest 2001; 108: 169-173.

[8] Yang H and Wang L. Heparan sulfate proteoglycans in cancer: pathogenesis and therapeutic potential. Adv Cancer Res 2023; 157: 251-291.

[9] Onyeisi JOS, Ferreira BZF, Nader HB and Lopes CC. Heparan sulfate proteoglycans as targets for cancer therapy: a review. Cancer Biol Ther 2020; 21: 1087-1094.

[10] Hayashida K, Aquino RS and Park PW. Coreceptor functions of cell surface heparan sulfate proteoglycans. Am J Physiol Cell Physiol 2022; 322: C896-C912.

[11] Roldán FL, Izquierdo L, Ingelmo-Torres M, Lozano JJ, Carrasco R, Cuñado A, Reig O, Mengual L and Alcaraz A. Prognostic gene expression-based signature in clear-cell renal cell carcinoma. Cancers (Basel) 2022; 14: 3754.

[12] Roldán FL, Lozano JJ, Ingelmo-Torres M, Carrasco R, Díaz E, Ramirez-Backhaus M, Rubio J, Reig O, Alcaraz A, Mengual L and Izquierdo L. Clinicopathological and molecular prognostic classifier for intermediate/high-risk clear cell renal cell carcinoma. Cancers (Basel) 2021; 13: 6338.

[13] Zhang Y, Yu Y, Cao X and Chen P. Role of lncRNA FAM83H antisense RNA1 (FAM83H-AS1) in the progression of non-small cell lung cancer by regulating the miR-545-3p/heparan sulfate 6-O-sulfotransferase (HS6ST2) axis. Bioengineered 2022; 13: 6476-6489.

[14] Hatabe S, Kimura H, Arao T, Kato H, Hayashi H, Nagai T, Matsumoto K, DE Velasco M, Fujita Y, Yamanouchi G, Fukushima M, Yamada Y, Ito A,

Okuno K and Nishio K. Overexpression of heparan sulfate 6-O-sulfotransferase-2 in colorectal cancer. Mol Clin Oncol 2013; 1: 845-850.
[15] Song K, Li Q, Peng YB, Li J, Ding K, Chen LJ, Shao CH, Zhang LJ and Li P. Silencing of hHS6ST2 inhibits progression of pancreatic cancer through inhibition of notch signalling. Biochem J 2011; 436: 271-282.
[16] Cole CL, Rushton G, Jayson GC and Avizienyte E. Ovarian cancer cell heparan sulfate 6-O-sulfotransferases regulate an angiogenic program induced by heparin-binding epidermal growth factor (EGF)-like growth factor/EGF receptor signaling. J Biol Chem 2014; 289: 10488-10501.
[17] Pollari S, Käkönen RS, Mohammad KS, Rissanen JP, Halleen JM, Wärri A, Nissinen L, Pihlavisto M, Marjamäki A, Perälä M, Guise TA, Kallioniemi O and Käkönen SM. Heparin-like polysaccharides reduce osteolytic bone destruction and tumor growth in a mouse model of breast cancer bone metastasis. Mol Cancer Res 2012; 10: 597-604.
[18] Li S, Shen H, Wan Q, Chen P, Shu C, Wang H and Zhu W. Downregulation of HS6ST2 inhibits cervical cancer cell migration and invasion in vivo and in vitro. Discov Med 2023; 35: 1147-1159.
[19] Jin Y, He J, Du J, Zhang RX, Yao HB and Shao QS. Overexpression of HS6ST2 is associated with poor prognosis in patients with gastric cancer. Oncol Lett 2017; 14: 6191-6197.
[20] Petryszyn P, Chapelle N and Matysiak-Budnik T. Gastric cancer: where are we heading? Dig Dis 2020; 38: 280-285.
[21] Rawla P and Barsouk A. Epidemiology of gastric cancer: global trends, risk factors and prevention. Prz Gastroenterol 2019; 14: 26-38.
[22] Tyczyńska M, Kędzierawski P, Karakuła K, Januszewski J, Kozak K, Sitarz M and Forma A. Treatment strategies of gastric cancer-molecular targets for anti-angiogenic therapy: a state-of-the-art review. J Gastrointest Cancer 2021; 52: 476-488.
[23] Zeng Y and Jin RU. Molecular pathogenesis, targeted therapies, and future perspectives for gastric cancer. Semin Cancer Biol 2022; 86: 566-582.
[24] Di Maro G, Orlandella FM, Bencivenga TC, Salerno P, Ugolini C, Basolo F, Maestro R and Salvatore G. Identification of targets of Twist1 transcription factor in thyroid cancer cells. J Clin Endocrinol Metab 2014; 99: E1617-1626.
[25] Gao F, Liu S, Wang J, Wei G, Yu C, Zheng L, Sun L, Wang G, Sun Y, Bao Y and Song Z. TSP50 facilitates breast cancer stem cell-like properties maintenance and epithelial-mesenchymal transition via PI3K p110α mediated activation of AKT signaling pathway. J Exp Clin Cancer Res 2024; 43: 201.
[26] Bin L, Lin H and Jian R. PKMYT1 promotes epithelial-mesenchymal transition process in triple-negative breast cancer by activating notch signaling. Rev Invest Clin 2024; 76: 45-59.
[27] Lu C, Fan X, Zheng M, Zhang S, Wang P, Wang Y and Zhang S. GDF6 in gastric cancer upregulated by helicobacter pylori induces epithelial-mesenchymal translation via the TGF-β/SMAD3 signaling pathway. Pathol Res Pract 2024; 260: 155384.
[28] Emile MH, Emile SH, El-Karef AA, Ebrahim MA, Mohammed IE and Ibrahim DA. Association between the expression of epithelial-mesenchymal transition (EMT)-related markers and oncologic outcomes of colorectal cancer. Updates Surg 2024; 76: 2181-2191.
[29] Liu F, Wang Q, Wang Z, Zhang S, Ni Q and Chang H. ETV4 promotes the progression of cholangiocarcinoma by regulating glycolysis via the TGF-β signaling. Transl Oncol 2024; 47: 102035.
[30] Su Q, Wang JJ, Ren JY, Wu Q, Chen K, Tu KH, Zhang Y, Leong SW, Sarwar A, Han X, Zhang M, Dai WF and Zhang YM. Parkin deficiency promotes liver cancer metastasis by TMEFF1 transcription activation via TGF-β/Smad2/3 pathway. Acta Pharmacol Sin 2024; 45: 1520-1529.
[31] Zhu W and Dong C. Poly-L-Lactic acid increases collagen gene expression and synthesis in cultured dermal fibroblast (Hs68) through the TGF-β/Smad pathway. J Cosmet Dermatol 2023; 22: 1213-1219.
[32] Yang K, Xie Y, Xue L, Li F, Luo C, Liang W, Zhang H, Li Y, Ren Y, Zhao M, Wang W, Liu J, Shen X, Zhou W, Fei J, Chen W, Gu W, Wang L, Li F and Hu J. M2 tumor-associated macrophage mediates the maintenance of stemness to promote cisplatin resistance by secreting TGF-β1 in esophageal squamous cell carcinoma. J Transl Med 2023; 21: 26.
[33] Zhang Y, Zheng W, Zhang L, Gu Y, Zhu L and Huang Y. LncRNA FBXO18-AS promotes gastric cancer progression by TGF-β1/Smad signaling. Eur J Histochem 2023; 67: 3667.
[34] Zhang Y, Wang B, Song H and Han M. GLIS3, a novel prognostic indicator of gastric adenocarcinoma, contributes to the malignant biological behaviors of tumor cells via modulating TGF-β1/TGFβR1/Smad1/5 signaling pathway. Cytokine 2023; 170: 156342.
[35] Yuan XN, Liu Q, Shao YC, Guan XQ, Yang ZL, Chu MF, Zhang JW, Tian YH and Wei L. Mettl3 synergistically regulates TGF-β/SMAD2/3 to promote proliferation and metastasis of gastric cancer. Am J Cancer Res 2023; 13: 3185-3202.

Table S1. Target sequence of HS6ST2 siRNAs

siRNA	Target sequence
HS6ST2 (human) siRNA-1	AGGUAGACUUCGACAUCAA
	UUGAUGUCGAAGUCUACCU
HS6ST2 (human) siRNA-2	CCGUGAUCGUCCUCCAAUA
	UAUUGGAGGACGAUCACGG
HS6ST2 (human) siRNA-3	CCGCGUGGGUCAGAAGAAA
	UUUCUUCUGACCCACGCGG